Catalysis Today 171 (2011) 79–83

Contents lists available at ScienceDirect

Catalysis Today

journal homepage: www.elsevier.com/locate/cattod

# Optimal design of a $CH_4$ CPO-reformer with honeycomb catalyst: Combined effect of catalyst load and channel size on the surface temperature profile

Alessandra Beretta*, Alessandro Donazzi, Dario Livio, Matteo Maestri, Gianpiero Groppi, Enrico Tronconi, Pio Forzatti

*Laboratory of Catalysis and Catalytic Processes, Dipartimento di Energia, Politecnico di Milano, Piazza Leonardo da Vinci 32, 20 133 Milano, Italy*

ARTICLE INFO

*Article history:*
Received 26 November 2010
Received in revised form 23 February 2011
Accepted 29 March 2011
Available online 31 May 2011

*Keywords:*
Catalytic partial oxidation
Methane
Rhodium
Optimal design
Hot-spot temperature
Microkinetic model
Spatially resolved measurements
Transport phenomena

ABSTRACT

Previous experimental and modeling work on the short contact time catalytic partial oxidation (CPO) of $CH_4$ to syngas [1] pointed out that a key issue (and a weakness) of the process is represented by the hot spot that establishes on the catalyst surface at the reactor inlet. In this work, we show that the interplay between surface chemistry and mass transfer can be exploited to minimize the extent of surface hot-spots. By increasing the channel diameter and the catalyst load of a Rh-coated honeycomb monolith, we obtained a reduction of the rate of $O_2$ conversion (mass-transfer limited) and a selective enhancement of the rate of $CH_4$ conversion through endothermic reactions. The resulting temperature profile was significantly flatter. Detailed model analysis and spatially resolved temperature and concentration profiles within the honeycomb channels demonstrate the concept.

## 1. Introduction

In previous works [1,2], we addressed a theoretical and experimental investigation on the behavior of short contact time $CH_4$-CPO reformers, operating with Rh-coated honeycomb monoliths. Emphasis was given to the characterization of the reactor thermal behavior; this is the result of a complex coupling between chemical reactions and heat and mass transfer phenomena. It was shown that longitudinal temperature profiles are characterized by a pronounced hot-spot at the reactor inlet, with a sharp peak at the surface and a smoother maximum in the gas-phase. The shape of the surface temperature profile is due to the rapid $O_2$ consumption (fully mass transfer controlled) and thus to the localized heat release which occurs at the very reactor inlet; this is partly balanced by the heat consumption driven by the reforming reactions which are "spread" along the whole monolith length and give rise to syngas formation. Most of these results have been confirmed by the independent analysis of the performance of Rh-coated foams where the intensity of surface and gas-phase hot spots, the importance of $O_2$ mass transfer limitations and the evolution of the process stoichiometry along the axial reactor coordinate have been experimentally demonstrated by means of spatially resolved temperature and concentration measurements [3–6] and fully supported by the theoretical analyses [7,8].

Most importantly, the experimental investigation with honeycomb monoliths clearly showed that, at very high flow rates and in the presence of preheating (conditions that favor the onset of surface temperatures as high as 1000 °C), the CPO reformer showed an unstable thermal behavior. Progressively increasing temperatures were measured in the inlet reactor portion at first, and then, run after run, also downstream. The modeling analysis showed that the reactor heating could be explained by a progressive loss of activity; such loss was more important where the highest temperatures were reached. Such loss little affects the conversion of $O_2$, while strongly influences the rate of the more chemically controlled reforming reactions (note that the same phenomenology has been observed in the case of S-poisoned catalysts [9,10]).

Thus we believe that thermal management is of the utmost importance for the successful and durable operation of a $CH_4$-CPO reformer. Previously proposed guidelines for optimizing the reactor design (and minimizing the surface hot-spot temperature) are herein explored by the experimental demonstration and the theoretical analysis. At this scope state of the art tools for the diagnosis and analysis of the reactor performance have been adopted; these include spatially resolved sampling techniques (for the measurements of the solid and the gas-phase temperature, and of

---

* Corresponding author.
*E-mail address:* alessandra.beretta@polimi.it (A. Beretta).

0920-5861/$ – see front matter © 2011 Elsevier B.V. All rights reserved.
doi:10.1016/j.cattod.2011.03.081

the gas-phase composition) for the experimental investigation and detailed kinetic modeling for the theoretical analysis.

## 2. Experimental and theoretical tools

### 2.1. Catalytic materials

$CH_4$ CPO tests were performed over a 2 wt% Rh/α-$Al_2O_3$ catalyst supported honeycomb monoliths The catalyst powders were prepared by incipient wetness impregnation of α-$Al_2O_3$ (10 $m^2$/g surface area) with an aqueous solution of $Rh(NO_3)_3$. The catalyst was deposited onto the honeycomb support by dipping it into a slurry of the powders (prepared according to a standard recipe [11]) and blowing of the excess. To fix the slurry on the support surface, the coated honeycomb was flash-dried at 280 °C in air for 10 min. The catalyst load was estimated by weight difference before and after coating the monoliths with the catalyst. The thickness of the layer (10–50 μm) was calculated by assuming a washcoat density of 1.4 g/$cm^3$. The dispersion of Rh was estimated by pulse chemisorption of $H_2$ and CO performed over powder samples aged under representative conditions [12], and was equal to 20% according to both techniques.

Concerning the supports, 400 cpsi (1.09 mm channel opening) and 115 cpsi (1.88 mm channel opening) ceramic honeycomb monoliths were used.

### 2.2. Lab-scale reactor

The experimental investigation was performed by means of an adiabatic CPO reformer operating at high flow rates (5–20 Nl/min). The reactor is a stainless steel tube with an internal quartz lining that prevents C formation. Great care was given to the thermal insulation so that the experiments could be rigorously representative of an adiabatic behavior, a desired condition both for the sake of reproducibility and for guaranteeing the adequacy of the modeling analysis. Also, this was considered the correct condition for a fair evaluation of the effects, herein examined, of channel size and catalyst load on the shape of the temperature profiles. Thus, in the case of the 400 cpsi support, the monolith dipping procedure was realized in such a way that an initial length of 0.5 cm remained uncoated. In a companion paper [13], we have shown that the presence of a short inert inlet monolith portion preserves at the best the adiabaticity of the monolith in the presence of high hot spot temperatures at the catalyst inlet. Instead, the presence of an inert portion before the catalytic monolith does not affect the adiabatic character of a catalytic monolith whose inlet hot spots are negligible (which was, as shown in the following, the case of the 115 cpsi monolith). The internal reactor layout consisted of the honeycomb monolith (with the catalytic portion downstream of the inert one) in between an upstream FeCrAlloy foam, kept at about 1 cm distance, and a downstream uncoated honeycomb monolith, which act as thermal radiation shields and flow mixers. Thermal insulation was also obtained by wrapping the static mixer, the lines upstream of the reactor and the reactor with a very thick layer of quartz wool taping. Indeed, the experiments herein reported are representative of a fully adiabatic behavior; the temperatures that were measured at the outlet section of the tested monoliths equaled in fact the expected theoretical adiabatic temperatures.

The setup used for collecting spatially resolved concentration and temperature profiles is similar to the one introduced and extensively described in papers from Schmidt and co-workers [6]. The sampling system consisted of a capillary of small diameter (O.D. = 340 μm, I.D. = 200 μm) that was moved within a central channel of the honeycomb monolith by means of a linear actuator. The gases were sampled through the capillary tip and pumped to a micro gas chromatograph.

For the measurement of either the axial temperature profile of the gas and the solid phase, an analogous capillary (O.D. = 670 μm, I.D. = 530 μm) sealed at one end was used. This served as inert sleeve for the axial movement of a thin K-type thermocouple (ø = 250 μm) or an optical fiber (ø = 330 μm) with a 45° polished tip connected to a narrow-band infrared pyrometer (Impac Infrared, IGA 5-LO). The measuring transducer included the lens system, the IR detector and the signal processor. The IR detector was an Indium–Gallium–Arsenic photodiode, sensitive to radiation in the wavelength range 1.45–1.8 μm. The output voltage was calibrated between 350 and 1100 °C. It is important to note that the signal of the pyrometer is affected by artifacts at the boundary of the monolith (e.g. the measurement of high temperatures before the catalytic monolith and the sudden drop of temperature close to the exit monolith section), due to the fact that the optical fiber tip tends to collect some light also from zones in front of it. These phenomena, already recognized by Donazzi et al. [8], do not influence significantly the temperature measurement within the monolith channel, as will be shown in a future work, dedicated to the analysis of the pyrometer signal in honeycomb reactors.

### 2.3. Reactor model and kinetic scheme

The experiments were analyzed by means of a 1D, heterogeneous, dynamic, fixed bed reactor model [2]. The model consists of mass, energy and momentum balances for the gas-phase and the solid phase, which includes axial convection and diffusion, solid conduction and gas–solid transport terms. Model equations are reported in Table 1 of [2,14]. Gas-phase reactions were accounted for using the detailed scheme of Ranzi et al. [15]. In line with Ref. [16], no contribution from homogeneous chemistry was found under our operating conditions. Heat conduction in the solid was described with an effective axial thermal conductivity coefficient corrected by addition of radiation. The thermal conductivity of the cordierite support was taken as 2.5 W/(m K). Radiative dispersion effects at the back and front heat shield were introduced in the boundary conditions.

The model incorporates a thermodynamically consistent $C_1$ microkinetic scheme [17,18] for the conversion of $CH_4$ to syngas over Rh, consisting of 82 surface reactions and 13 adspecies. It has been derived using a hierarchical multiscale methodology involving both semi-empirical methods (UBI-QEP) and first principle techniques [17,19]. The scheme was validated over a wide set of $CH_4$ CPO experimental data within an annular microreactor under quasi-isothermal conditions [20,21]. The resulting scheme was able to describe several reacting systems, namely $CH_4$ pyrolysis and oxidation, steam reforming, $H_2$- and CO-rich oxidation, WGS and reverse WGS.

Concerning heat and mass transfer in the honeycomb monolith channels, the correlation for the local Sherwood and Nusselt numbers from [22] were applied, assuming the Chilton–Colburn analogy.

## 3. Results and discussion

### 3.1. Thermal behavior and performance of a reference honeycomb monolith

Fig. 1 shows the complete characterization of the performance of a “standard” honeycomb monolith, with 400 cpsi cell density, 250 mg catalyst load, operated under adiabatic conditions. The measured temperature profiles clearly indicated the presence of

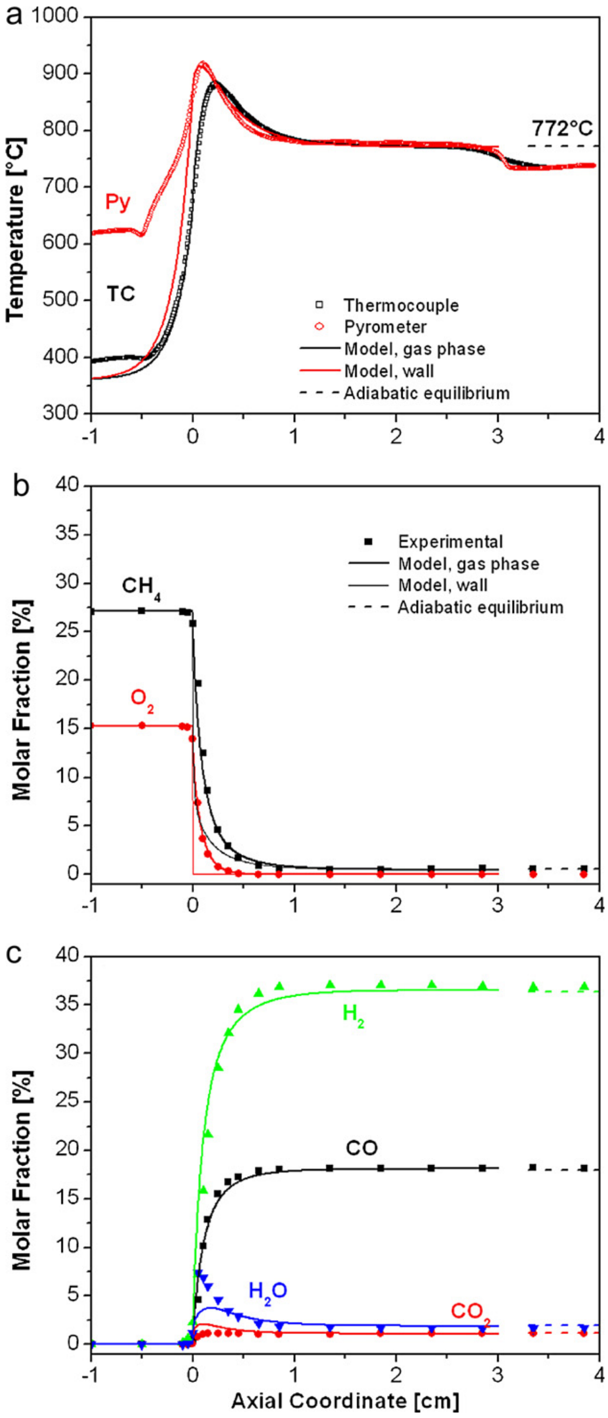

**Fig. 1.** (a) Temperature measurements in 400 cpsi honeycomb monolith; (b) concentration profiles of reactants; (c) concentration profiles of products. Operating conditions: $CH_4$/air mixture with 10 Nl/min total flow rate and $O_2/C = 0.54$; inlet gas temperature = 362 °C, atmospheric pressure. Symbols: experimental measurement. Solid lines: model predictions. Dotted lines: calculated concentration at the wall of $O_2$ and $CH_4$. Dashed lines at the right end-side of the panels = thermodynamic equilibrium.

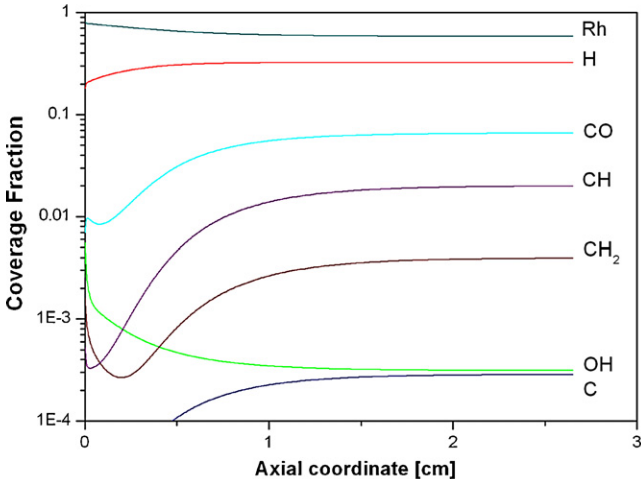

**Fig. 2.** Surface coverages calculated by the model. Operating conditions as in Fig. 1.

a hot spot that developed along the inlet zone, 1 cm long; the optical pyrometer showed a maximum temperature of about 930 °C, while the sliding thermocouple measured a maximum temperature of about 870 °C, few mm apart. Both the temperature profiles became relatively flat downstream of the hot-spot, thus suggesting that thermodynamic equilibrium was reached and that the 3 cm long monolith was largely oversized at this high flow rate. Concerning the measured concentration profiles, it was found that $O_2$ conversion was complete within 5 mm from the catalyst entrance. Also methane was consumed at a great extent within the same short length; at 5 mm, the measured methane conversion was about 93%, but it further increased up to 97% few millimeters downstream. The measurement of the product distribution showed that hydrogen and CO were produced from the very entrance and syngas production grew rapidly along the axial coordinate (mostly within the first 5 mm); also water was rapidly formed at the very entrance but its concentration passed through a narrow peak (with a maximum located at about 1 mm from the inlet section) and then also rapidly decreased to a low outlet concentration. $CO_2$ was also formed in small amounts. The measured outlet concentrations are in complete agreement with the thermodynamic equilibrium (that is represented by the dashed lines at the right end side of Fig. 1). An overall analysis of these results tells that the catalyst formulation was extremely active and a good overlay between exothermic and endothermic reactions was realized, since within the short length where $O_2$ was consumed, most of syngas was also formed. Still the occurrence of a hot-spot was clearly detected.

Fig. 1 reports the model predictions in solid lines. Catalyst and gas phase temperatures were predicted in close agreement with the experimental evidence. In agreement with the experimental data, the calculated $O_2$ conversion was complete within 5 mm length and $CH_4$ conversion was predicted to reach the equilibrium within a longer monolith portion. The distribution of products was also nicely described. As already discussed in previous papers from this and other laboratories [7,8], and shown by the thin solid lines in Fig. 1, the calculated concentration of $O_2$ at the wall dropped to zero at the very inlet of the catalytic monolith. This is the evidence that $O_2$ consumption was fully controlled by external mass transfer; as recently illustrated for Rh-coated foams [7], also in the case of honeycomb channels such a condition is reached because of the extremely high rate of the reaction steps consuming O* species, and especially that of the $H^* + O^* \rightarrow OH^*$ step. The most important consequence of the diffusion controlled conversion of $O_2$ is that the surface coverage of O* is practically zero, and the activation and consumption of methane occurs through a pyrolytic route (i.e. the abstraction of H* from $CH_X$ intermediates is not oxygen assisted [17]). Fig. 2 shows the calculated surface coverages of reacting species along the axial coordinate: at these high temperatures, the Rh surface is relatively clean and H* and CO* are the most abundant adsorbed intermediates.

### 3.2. Optimization strategies

In a previous modeling analysis [1], the interplay between diffusion phenomena and chemical process at the wall has been discussed in detail. In the modeling analysis we explored the ways in which such interplay can be exploited in order to flatten the inlet temperature profiles, optimize the thermal behavior of the reactor and eventually enhance the lifetime of the catalyst. For the sake of clarity, some important conclusions of that analysis are herein summarized.

Since $O_2$ conversion is kinetically controlled by gas-solid diffusion while $CH_4$ conversion is more kinetically controlled by the surface chemistry, the channel opening and the catalyst load are sensitive design parameters. The enlargement of the channel diameter from 1 to 3 mm at constant catalyst fraction was estimated to decrease effectively the surface hot-spot temperature. In fact, the increase of the channel diameter reduces the local rate of $O_2$ consumption (through the reduction of the mass transfer coefficient) while it affects at a lesser extent the rate of $CH_4$ consumption. Conversely, an increase of the catalyst reactivity (e.g. of Rh site density) has no effect on the rate of $O_2$ consumption, but has an important promoting effect on the rate of $CH_4$ consumption. In both cases, the expected final result is a more favorable balancing between exothermic and endothermic reactions and a moderation of the surface hot-spot.

### 3.3. Experimental validation: combined effect of increased channel size and catalyst load

Fig. 3 shows the measured performance of a Rh-coated honeycomb monolith which has been designed along the optimal criteria above summarized. The 110 cpsi support was characterized by a channel opening of about 2 mm and the catalyst load amounted to about 750 mg, that is three times the catalyst load of the reference monolith previously tested.

The measured composition profiles indicated that in the new honeycomb monolith the $O_2$-consumption length increased significantly, passing from 5 mm to over 10 mm. Model predictions, also reported in Fig. 2 as solid lines, describe very nicely the experimental data and show that the more sluggish trend of $O_2$ concentration profile is completely explained by the reduced rate of gas-phase mass transfer in the wider honeycomb channels. At the same time, the increased amount of catalyst fraction in the reactor kept high the conversion rate of $CH_4$, the syngas yield and the heat consumption rate. As a final result, the measured and predicted temperature profiles on the catalyst surface and in the bulk phase were dramatically smoother (almost gradientless) and characterized by over 120 °C reduction of the maximum temperature in both phases.

## 4. Concluding remarks

The elimination of surface hot-spots is a prerequisite for the durable and stable operation of short contact time $CH_4$-CPO reformers. Once recognized the key role of mass transfer limitations on the thermal behavior of the autothermal reformer, modeling work clearly shows the potential offered by the reactor design. In this work we extend the theoretical analysis and give the experimental demonstration that the support geometry and the catalyst activity are sensitive parameters for achieving an optimal thermal behavior (in principle a gradientless temperature profile). By increasing almost two times the channel opening of the honeycomb support and three times the fraction of Rh in the reactor, the inlet rate of oxidation reactions was decreased and the $O_2$-consumption length (typically as short as few mm) penetrated well within the monolith while the yield to syngas was preserved. The adoption of the in situ sampling technique has been crucial to pursue the result and completely characterize the performance of the honeycomb monolith with enhanced thermal behavior.

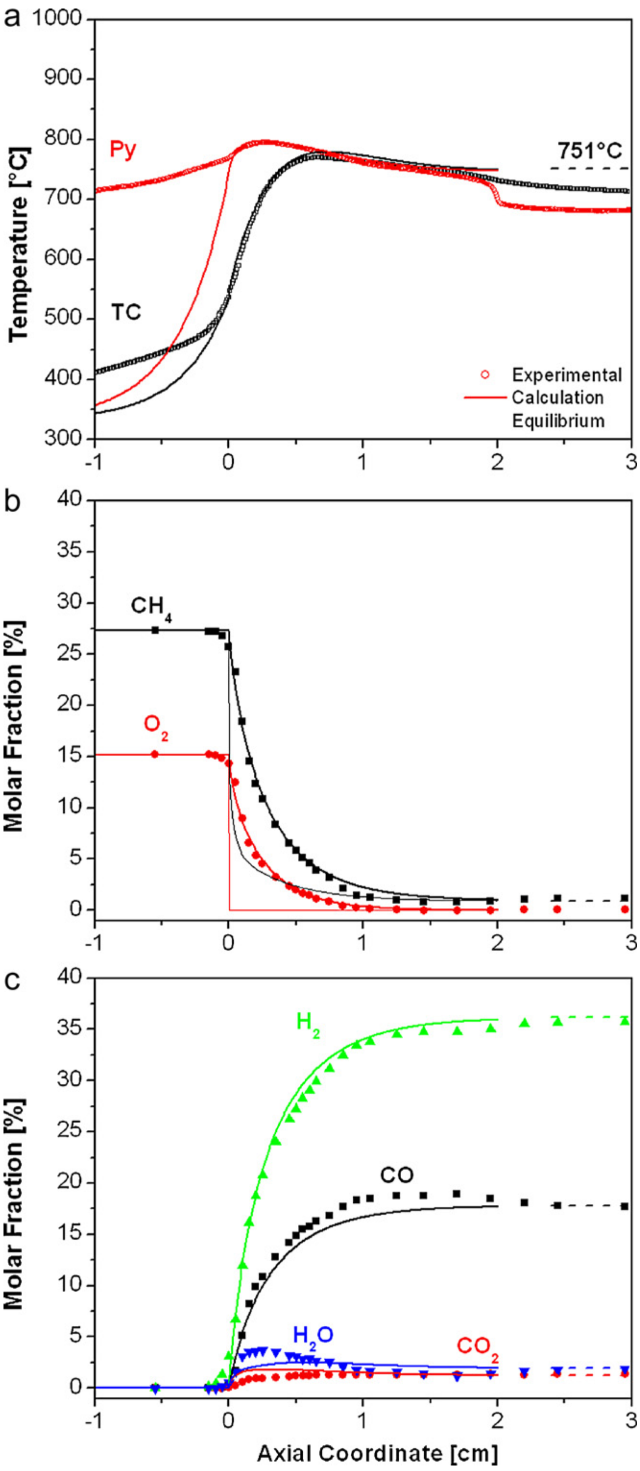

**Fig. 3.** (a) Temperature measurements in 115 cpsi honeycomb monolith; (b) concentration profiles of reactants; (c) concentration profiles of products. Operating conditions: $CH_4$/air mixture with 10 Nl/min total flow rate and $O_2/C = 0.54$; inlet gas temperature = 362 °C, atmospheric pressure. Symbols: experimental measurement. Solid lines: model predictions. Dotted lines: calculated concentration at the wall of $O_2$ and $CH_4$. Dashed lines at the right end-side of the panels = thermodynamic equilibrium.

## References

[1] A. Beretta, G. Groppi, M. Lualdi, I. Tavazzi, P. Forzatti, Experimental and modeling analysis of methane partial oxidation: transient and steady-state behavior of Rh-coated honeycomb monoliths, Industrial and Engineering Chemistry Research 48 (2009) 3825–3836.

[2] M. Maestri, A. Beretta, G. Groppi, E. Tronconi, P. Forzatti, Comparison among structured and packed-bed reactors for the catalytic partial oxidation of $CH_4$ at short contact times, Catalysis Today 105 (2005) 709–717.

[3] A. Donazzi, B.C. Michael, L.D. Schmidt, Chemical and geometric effects of Ce and washcoat addition on catalytic partial oxidation of $CH_4$ on Rh probed by spatially resolved measurements, Journal of Catalysis 260 (2008) 270–275.

[4] R. Horn, N.J. Degenstein, K.A. Williams, L.D. Schmidt, Spatial and temporal profiles in millisecond partial oxidation processes, Catalysis Letters 110 (2006) 169–178.

[5] R. Horn, K.A. Williams, N.J. Degenstein, A. Bitsch-Larsen, D. Dalle Nogare, S.A. Tupy, L.D. Schmidt, Methane catalytic partial oxidation on autothermal Rh and Pt foam catalysts: oxidation and reforming zones, transport effects, and approach to thermodynamic equilibrium, Journal of Catalysis 249 (2007) 380–393.

[6] B.C. Michael, A. Donazzi, L.D. Schmidt, Effects of $H_2O$ and $CO_2$ addition in catalytic partial oxidation of methane on Rh, Journal of Catalysis 265 (2009) 117–129.

[7] D. Dalle Nogare, N.J. Degenstein, R. Horn, P. Canu, L.D. Schmidt, Modeling spatially resolved profiles of methane partial oxidation on a Rh foam catalyst with detailed chemistry, Journal of Catalysis 258 (2008) 131–142.

[8] A. Donazzi, M. Maestri, B.C. Michael, A. Beretta, P. Forzatti, G. Groppi, E. Tronconi, L.D. Schmidt, D.G. Vlachos, Microkinetic modeling of spatially resolved autothermal $CH_4$ catalytic partial oxidation experiments over Rh-coated foams, Journal of Catalysis 275 (2010) 270–279.

[9] A. Bitsch-Larsen, N.J. Degenstein, L.D. Schmidt, Effect of sulfur in catalytic partial oxidation of methane over Rh–Ce coated foam monoliths, Applied Catalysis B: Environmental 78 (2008) 364–370.

[10] S. Cimino, R. Torbati, L. Lisi, G. Russo, Sulphur inhibition on the catalytic partial oxidation of methane over Rh-based monolith catalysts, Applied Catalysis A: General 360 (2009) 43–49.

[11] M. Valentini, G. Groppi, C. Cristiani, M. Levi, E. Tronconi, P. Forzatti, The deposition of gamma-$Al_2O_3$ layers on ceramic and metallic supports for the preparation of structured catalysts, Catalysis Today 69 (2001) 307–314.

[12] A. Beretta, A. Donazzi, G. Groppi, P. Forzatti, V. Dal Santo, L. Sordelli, V. De Grandi, R. Psaro, Testing in annular micro-reactor and characterization of supported Rh nanoparticles for the catalytic partial oxidation of methane: effect of the preparation procedure, Applied Catalysis B – Environmental 83 (2008) 96–109.

[13] D. Livio, A. Donazzi, A. Beretta, G. Groppi, P. Forzatti, Optimal design of a CPO-reformer of light hydrocarbons with honeycomb catalyst: effect of frontal heat dispersions on the temperature profiles, Topics in Catalysis, submitted for publication.

[14] I. Tavazzi, M. Maestri, A. Beretta, G. Groppi, E. Tronconi, P. Forzatti, Steady-state and transient analysis of a $CH_4$-catalytic partial oxidation reformer, AIChE Journal 52 (2006) 3234–3245.

[15] E. Ranzi, A. Sogaro, P. Gaffuri, G. Pennati, T. Faravelli, Wide range modeling study of methane oxidation, Combustion Science and Technology 96 (1994) 279–325.

[16] R. Schwiedernoch, S. Tischer, C. Correa, O. Deutschmann, Experimental and numerical study on the transient behavior of partial oxidation of methane in a catalytic monolith, Chemical Engineering Science 58 (2003) 633–642.

[17] M. Maestri, D.G. Vlachos, A. Beretta, G. Groppi, E. Rronconi, A C-1 microkinetic model for methane conversion to syngas on $Rh/Al_2O_3$, AIChE Journal 55 (2009) 993–1008.

[18] A.B. Mhadeshwar, H. Wang, D.G. Vlachos, Thermodynamic consistency in microkinetic development of surface reaction mechanisms, Journal of Physical Chemistry B 107 (2003) 12721–12733.

[19] A.B. Mhadeshwar, D.G. Vlachos, Hierarchical, multiscale surface reaction mechanism development: CO and $H_2$ oxidation, water–gas shift, and preferential oxidation of CO on Rh, Journal of Catalysis 234 (2005) 48–63.

[20] A Donazzi, A. Beretta, G. Groppi, P. Forzatti, Catalytic partial oxidation of methane over a 4% $Rh/\alpha\text{-}Al_2O_3$ catalyst, Part I: kinetic study in annular reactor, Journal of Catalysis 255 (2008) 241–258.

[21] A. Donazzi, A. Beretta, G. Groppi, P. Forzatti, Catalytic partial oxidation of methane over a 4% $Rh/\alpha\text{-}Al_2O_3$ catalyst, Part II: role of $CO_2$ reforming, Journal of Catalysis 255 (2008) 259–268.

[22] R.K. Shah, A.L. London, Laminar Flow Forced Convection in Ducts, Academic Press, New York, 1978.